

RESEARCH

Open Access



Potential contribution of early endothelial progenitor cell (eEPC)-to-macrophage switching in the development of pulmonary plexogenic lesion

Feng-Jin Shao^{1,2,3†}, Xiao-Ling Guo^{4†}, Jia-Xue Xu^{1,5}, Rui Liu^{1,2,3}, Dan-Yue Li¹, Qing-Hao Li¹, Ting Zhou¹, Cun Fang¹ and Xun Tan^{1,2,3*}

Abstract

Background: Plexiform lesions, which have a dynamic appearance in structure and cellular composition, are the histological hallmark of severe pulmonary arterial hypertension in humans. The pathogenesis of the lesion development remains largely unknown, although it may be related to local inflammation and dysfunction in early progenitor endothelial cells (eEPCs). We tested the hypothesis that eEPCs contribute to the development of plexiform lesions by differentiating into macrophages in the setting of chronic inflammation.

Methods: The eEPC markers CD133 and VEGFR-2, macrophage lineage marker mannose receptor C-type 1 (MRC1), TNF α and nuclear factor erythroid 2-related factor 2 (Nrf2) in plexiform lesions in a broiler model were determined by immunohistochemistry. eEPCs derived from peripheral blood mononuclear cells were exposed to TNF α , and macrophage differentiation and angiogenic capacity of the cells were evaluated by phagocytotic and Matrigel plug assays, respectively. The role of Nrf2 in eEPC-to-macrophage transition as well as in MRC1 expression was also evaluated. Intratracheal installation of TNF α was conducted to determine the effect of local inflammation on the formation of plexiform lesions.

Results: Cells composed of the early lesions have a typical eEPC phenotype whereas those in more mature lesions display molecular and morphological characteristics of macrophages. Increased TNF α production in plexiform lesions was observed with lesion progression. In vitro studies showed that chronic TNF α challenge directed eEPCs to macrophage differentiation accompanied by hyperactivation of Nrf2, a stress-responsive transcription factor. Nrf2 activation (Keap1 knockdown) caused a marked downregulation in CD133 but upregulation in MRC1 mRNA. Dual luciferase reporter assay demonstrated that Nrf2 binds to the promoter of MRC1 to trigger its expression. In good agreement with the in vitro observation, TNF α exposure induced macrophage differentiation of eEPCs in Matrigel plugs, resulting in reduced neovascularization of the plugs. Intratracheal installation of TNF α resulted in a significant increase in plexiform lesion density.

[†]Feng-Jin Shao and Xiao-Ling Guo contributed equally to this work and should be considered co-first authors

*Correspondence: tanxun@zju.edu.cn

¹ Department of Veterinary Medicine, Zhejiang University, Hangzhou 310058, People's Republic of China

Full list of author information is available at the end of the article



Conclusions: This work provides evidence suggesting that macrophage differentiation of eEPCs resulting from chronic inflammatory stimulation contributes to the development of plexiform lesions. Given the key role of Nrf2 in the phenotypic switching of eEPCs to macrophages, targeting this molecular might be beneficial for intervention of plexiform lesions.

Keywords: Pulmonary arterial hypertension, Pulmonary arterial pressure, Plexiform lesion, Nuclear factor erythroid 2-related factor 2, Endothelial progenitor cells, Phenotypic switching, Inflammation, Macrophage, Keap1

Introduction

Plexiform lesions are a predominant histological feature in humans suffering from severe pulmonary arterial hypertension (PAH), including idiopathic PAH (IPAH), ultimately leading to vascular occlusion [1, 2]. These structures are typically located at an arterial branch point or at the origin of a supernumerary artery, and are considered to be functionally important because it could completely occlude the vessel lumen of the affected vessels [2]. It is believed that patients tend to be unresponsive to vasodilator therapy and have an extremely poor prognosis when plexogenic arteriopathy is present [3].

The cause and origins of plexiform lesions remain largely unclear. Several mechanisms have been proposed, involving inflammation mechanisms and disordered angiogenesis [4–7]. In recent years, endothelial progenitor cells (EPCs) have attracted increasing interest in vascular physiology and pathophysiology [8]. To date, two distinct types of EPCs have been described: the early EPCs (eEPCs, also termed circulating angiogenic cells [ASC] or colony-forming unit-endothelial cells) derived from the bone marrow and the late outgrowth EPCs (late EPCs) derived from nonhematopoietic tissue, presumably from tissue vascular niches [9–11]. A beneficial effect on endothelial repair after injury has, in particular, been shown for early EPCs [12, 13]. Based on more recent observations, however, it is suggested that dysfunction of eEPCs contributes to the formation of plexiform lesions in PAH patients [14–16], which was highlighted by evidence of eEPC accumulation in the sites of lesions. However, the exact mechanisms accounting for eEPC dysfunction and the fate of the EPCs in the sites of plexiform lesions remain to be fully elucidated.

In addition to eEPCs, monocytes/macrophages are also found in increase number within plexiform lesions of human PAH and in animal model with severe PAH [17]. However, it is of interest to note that eEPCs display a mixed macrophage/endothelial cell phenotype [18–20], suggesting complex relationships between eEPCs and monocytes/macrophages. While it is proposed that eEPCs with a mixed macrophage/endothelial cell phenotype can develop an endothelial-like cell phenotype under angiogenic conditions [21, 22], there is also evidence that inflammatory environment induces the

differentiation of eEPCs into immune/inflammatory cells by yet unknown mechanisms [23], leading to the suggestion that eEPC angiogenic commitment is not a definitive event and that the phenotype and function of these cells are affected by the local microenvironment. Given the intensive perivascular inflammation of plexiform lesions [7], we proposed that the impaired angiogenic activity of local eEPCs is associated with a phenotypic switching of eEPCs to macrophages. However, evidence supporting this hypothesis is still lacking.

A line of evidence shows that the function and fate of stem and progenitor cells are under redox regulation in physiologic and pathologic conditions [24, 25]. The inducible transcription factor Nrf2 (nuclear factor erythroid 2-related factor 2; encoded by *Nfe2l2* gene) is emerging as a central regulator of oxidative stress by activating a wide array of cytoprotective and antioxidant gene targets [26–29]. Although initially considered to function primarily for maintaining and regulating the cellular redox equilibrium, Nrf2 is now recognized to modulate various cellular processes including cell proliferation and differentiation [30]. Recent evidence shows that Nrf2 contributes to the pathogenesis of atherosclerosis via inducing the phenotypic changes of vascular cells as well as macrophages in the lesion [31, 32]. In this regard, Nrf2 may serve as a signaling mechanism to participate in the pathogenesis of plexiform lesions.

Although numerous experimental animal models of PAH have been developed, only few of them develop plexiform-like lesions (reviewed by Bonnet et al. 2017) [33]. In addition, attempts to better understand the pathogenesis of plexogenic arteriopathy in humans with severe PAH have been hampered by the absence of animal models in which plexiform lesions develop spontaneously [34]. Domesticated fast growing meat-type chickens (broiler chickens) are highly prone to idiopathic PAH (previously known as ascites syndrome; pulmonary hypertension syndrome) [35–37], and can spontaneously develop plexiform lesions in small pulmonary arteries exhibiting histological features similar to that seen in human PAH [38–40]. We have recently confirmed the presence of eEPCs (CD133+/VEGFR-2+ cells) and foam-like macrophages in the structures, and provided evidence that the lesion development in this avian model

is associated with hemodynamic stress [41, 42]. More recently, we showed that transplantation of mesenchymal stromal cells attenuates neointimal and plexogenic arteriopathy in PAH broiler chickens through modulating lung inflammation [43].

The aim of this work is to uncover the mechanisms by which inflammation and eEPCs conspire to cause the plexiform lesions in the avian model. We demonstrate here that chronic inflammation leads to the phenotypic switching of chicken eEPCs into macrophage lineage resulting in reduced angiogenic potential that involves the transcription factor Nrf2. Moreover, intratracheal instillation of proinflammatory cytokine tumor necrosis factor α (TNF α) promotes the development of plexiform lesions in broilers. This provides new insight into the mechanisms by which inflammation and eEPCs contribute to the plexogenic arteriopathy.

Materials and methods

Animal ethics

The animal experiments followed the National Guidelines for the Ethical Review of Laboratory Animal Welfare and were approved by the Ethics Committee of the Zhejiang University (ZJU20170554).

Animals

Cobb-500 broiler chickens with mixed sex were obtained at 1-day old from a local commercial hatchery (Hangzhou, China) and were reared at thermoneutral temperatures. They were fed a 21% crude protein corn-soybean meal-based broiler ration formulated to meet or exceed the NRC (1994) standards for all ingredients. Feed and water were supplied ad libitum.

Histology and immunohistochemistry

Birds at 4 weeks of age were humanely killed by cervical dislocation. The whole right lung was collected and cut in the transverse plane at the major rib indentations (costal sulci). For histological study, one inter-rib division from the middle of each lung was fixed in 4% paraformaldehyde. The apical regions of the left lungs were stored in liquid nitrogen until use. The paraffin-embedded blocks were serially cut in the transverse plane at 4–5 μm thickness. One slide of each lung was stained with haematoxylin and eosin (H&E). Number of plexiform lesions was counted for calculation of lesion density (number of lesions per section/ cm^2 per section).

The procedure for immunohistochemistry has been previously described [42]. Lung sections were incubated with mouse anti-chicken CD133 (self-prepared), rabbit anti-rat VEGFR-2 (Boster Biotechnology Technology, China), mouse anti-chicken monocyte/macrophage MRC1 (KUL-01, Southern Biotech, Birmingham,

USA), rabbit anti-human Nrf2 (Proteintech, Wuhan, China), or mouse anti-human TNF α (Huabio, Hangzhou, China) at a dilution of 1:50–1:200. The primary antibody detection was performed by using appropriate horseradish peroxidase (HRP)-conjugated secondary antibody and visualized with DAB (3,3'-diaminobenzidine tetrahydrochloride), followed by counterstaining with haematoxylin.

Ex vivo expansion of eEPCs

Ex vivo expansion of eEPCs were performed exactly as described in our previous work [44]. Briefly, mononuclear cell fraction of the peripheral blood (PBMC) from 4-week-old healthy birds was cultured in Endothelial cell growth medium (EGM)-2 (Lonza, Walkersvil, MD, USA) containing 2% fetal bovine serum (FBS), 100 U/ml penicillin, and 100 $\mu\text{g}/\text{ml}$ streptomycin at 39 °C in 5% CO_2 . Non-adherent cells were removed after 48 h. On day 4 of culture, cells were passaged using 0.25% trypsin/EDTA (Invitrogen) and plated on rat tail type 1 collagen-coated 6-well plates at 1×10^7 cells/well.

Cell viability assay

Cell viability was measured by using Cell Counting Kit-8 (CCK-8, FDBio Science, Hangzhou, China) according to the manufacturer's instructions. Briefly, eEPCs were seeded in 96-well plates at 1×10^4 cells/well in the presence or absence of r-TNF α (PeproTech Inc., Rocky Hill, NJ, USA). At the indicated time points, 10 μl of CCK8 solution was added into each well, followed by incubation of the plates at 39 °C in 5% CO_2 for 2 h. The optical density (OD) was measured at 450 nm.

Dil-ac-LDL and lectin staining

eEPCs were characterized by their ability to take up 1,1-dioctadecyl-3,3,3-tetramethylindocarbocyanine-labelled acetylated low-density lipoprotein (Dil-Ac-LDL) and bind to lectin (Ulex europaeus agglutinin, Sigma-Aldrich, Shanghai, China). A detailed protocol for Dil-Ac-LDL/lectin labeling has been described previously [45]. Cells were observed with a fluorescence microscope and photographed. The double-labelled cells were identified as eEPCs [46].

Immunocytochemistry (ICC)

Cells were fixed with 4% paraformaldehyde, followed by antigen retrieval (for MRC1) in Tris-EDTA buffer (pH 9.0) or permeabilization (for Nrf2 and CD133) in 0.1% Triton X-100 for 5–10 min. Nonspecific binding sites were blocked with 10% fetal bovine serum (FBS) for 20 min, followed by incubation with an anti-MRC1 (Southern Biotech, Birmingham, USA) used at a dilution of 1:50, anti-chicken CD133 (self-prepared) or anti-Nrf2

(Proteintech, Wuhan, China) at 1:200 overnight at 4 °C. The primary antibody detection was performed with an FITC-labeled or Alexa Fluor 568-conjugated secondary antibody (Abcam, Cambridge, UK). Nuclei were visualized with DAPI (4'-6-diamidino-2-phenylindole) for 5 min. Cells were observed with a fluorescence microscope and photographed. MRC1+ and CD133+ cells in each well were counted in 6 randomly selected high-power fields ($\times 200$).

Phagocytosis assay

eEPCs were cultured in 24-well plates at 3×10^5 cells/well with or without recombinant TNF α (r-TNF α ; 50 ng/ml) for 3–6 days. Cells were then marked with DAPI for 3 h before incubation with FITC-labeled *E. coli* DH5 α (1×10^9 CFU/ml) for another 3 h. Extracellular bacteria was killed by gentamicin. Cells that phagocytosed bacteria were counted in at least 6 randomly selected high-power fields ($\times 200$) under a fluorescence microscope. Broiler PBMNC-derived macrophages were used as a positive control.

In vivo Matrigel plug assay

Briefly, 6×10^5 eEPCs were treated with or without recombinant TNF α (r-TNF α ; 50 ng/ml) for 24 h and were mixed with 200 μ l Matrigel (BD Biosciences, San Jose, CA, USA). Thereafter, the Matrigel mixture was subcutaneously injected into 4-week-old broilers. Matrigel mixed only with r-TNF α was used as a blank control. After 6 days, the birds were killed and the Matrigel plugs were harvested, fixed in 4% formaldehyde and processed for histology and immunohistochemistry analyses.

Keap1 siRNA transfection

Chicken nontargeting negative control siRNAs (NC siRNA) and siRNA specific for the chicken Keap1 was designed and synthesized by GenePharma (Shanghai, China). Briefly, siRNA was complexed with LipofectamineTM 2000 (Invitrogen, Waltham, MA, USA) according to manufacturer's instructions before transfection. eEPCs were incubated with siRNA (final siRNA pool concentration of 20 nM) for 6 h in a humidified incubator. Knockdown efficiencies were determined by qPCR.

Real-time quantitative PCR assay

Total RNA was extracted from the cultured cells using TRIzol (Takara). The RNA was reverse transcribed with the PrimeScript RT reagent Kit with genomic DNA (gDNA) Eraser (Takara, Dalian, China). The 80–150-bp primers for each gene were purchased from Tsingke Biological technology (Additional file 1: Table S1). Quantitative assessment of target messenger RNA (mRNA) levels

was performed by qPCR using a SYBR-Green Quantitative PCR kit (Vazyme, Nanjing, China) with a Roche LightCycler 480 II system (Roche Diagnostics GmbH, Mannheim, German). The cycle threshold (Ct) values were normalized to the expression of two reference genes (*B2M*, *RPL19*). The relative expression of mRNA was calculated using a Pfaffl analysis method.

Protein extraction and Western blot analysis

Total protein extraction from lung tissues and cultured cells were performed by using a radioimmunoprecipitation assay buffer (RIPA) containing protease inhibitors and phosphatase inhibitors (FDBio Science, Hangzhou, China). Nuclear and cytoplasmic fractionation was conducted using a Nuclear-Cytosol Extraction Kit (FDBio Science, Hangzhou, China) according to the manufacturer's instructions. Samples were boiled at 99 °C for 5 min and then separated by using a sodium dodecyl sulfate (SDS)-10% polyacrylamide gel electrophoresis (PAGE) Fast Preparation Kit (FDBio Science, Hangzhou, China). After gel electrophoresis, the proteins from the gels were transferred to the 0.45 μ m PVDF membranes (Millipore, USA). The membranes were blocked in 5% non-fat milk for 2 h at room temperature and incubated with primary antibodies against Nrf2 (Proteintech, Wuhan, China), Keap1 (Proteintech, Wuhan, China), β -actin (Santa Cruz Biotechnology, Shanghai, China), histone (Santa Cruz Biotechnology, Shanghai, China) and tubulin (FDBio Science, Hangzhou, China) at a dilution of 1:1000 overnight at 4 °C. The primary antibody was detected by a horseradish peroxidase (HRP)-conjugated secondary antibody (FDBio Science, Hangzhou, China). Electrochemiluminescent (ECL, FDBio Science, Hangzhou, China) was used to visualize the immunoreactive bands.

Luciferase assay

The full-length open reading frame (ORF) of chicken Nrf2 cDNA with an optimal Kozak consensus sequence just before the in-frame first ATG was cloned into the eukaryotic expression vector pEGFP-C3 (pEGFP-C3-Nrf2). A predicted regulatory region containing 978 kb of a 5' flanking sequence (from – 45 to – 1022) of *MRC1* was cloned into the *Kpn* I and *Hind* III of pGL3-basic vector (Promega, Madison, Wisconsin, USA) containing a firefly luciferase reporter gene. The constructs were confirmed by DNA sequencing. The pRL-TK vector (Promega, Madison, Wisconsin, USA) containing a Renilla reniformis luciferase reporter gene was used as a control for transfection efficiency in the Dual-Luciferase Reporter Assay System. All plasmid DNAs were transfected into the HEK-293T cell line using the Lipo8000 (Beyotime Biotech, Nanjing, China). Luciferase activities were analyzed in 20 μ l cell lysates with the Dual Luciferase Assay

kit (Vazyme, Nanjing, China) on a BioTek Synergy H1 microplate reader (Winooski, Vermont, USA). The relative luciferase activities are expressed as a ratio of the pGL3 reporter activity to that of the control plasmid pRL.

Intratracheal instillation of TNF α

Intratracheal TNF α instillation was performed following a modified protocol described earlier for rat [47]. In brief, birds at 14 days of age were anesthetized by inhalation of diethyl ether and received twice either 100 μ l saline or 0.5 μ g recombinant TNF α in 100 μ l saline solution intratracheally, followed by another intratracheal instillation after 3 days. Birds were humanely killed 3 days after the second instillation. The hearts were removed, dissected, and weighed for calculation of the right-to-total ventricular weight ratio (RV/TV) as an indicator of pulmonary arterial hypertension [37]. Lung tissue was sampled as described above.

Statistical analysis

Data were analyzed for normality using Shapiro–Wilk test as a justification for using parametric analysis. Difference in cell proliferation was compared using one-way analysis of variance (ANOVA) followed by Bonferroni post-hoc test. Other data were analyzed using non-parametric Mann–Whitney U test due to the small sample size or not normally distributed. Data were expressed as mean \pm s.d. (ANOVA) or median \pm 95% confidence interval (Mann–Whitney). The software used was SPSS 22.0 for Window (IBM Corp., Armonk, NY, USA). Differences were considered significant at $P < 0.05$.

Results

Cells within the early and mature plexiform lesions demonstrate distinct molecular characteristics

To evaluate the cell phenotype in plexiform lesions at different differentiation stages, lung slides was examined to confirm the presence of plexiform lesions by H&E stain, and the expression of CD133, VEGFR-2 as well as mannose receptor C-type 1 (MRC1), was evaluated by immunohistochemistry analysis using serially cut slides. MRC1+ monocyte/macrophage lineage cells have been found to exhibit features similar to those in mammals [48]. As shown in Fig. 1, we determined strong expression of MRC1, CD133 and VEGFR-2 in cells within the early lesions indicative of the presence of a mixed macrophage/endothelial cell phenotype that has been defined as eEPCs. In more mature lesions foam-like macrophages became predominant, which demonstrated weak CD133 reactivity but strong expression in MRC1 and VEGFR-2, resembling differentiated, polarized macrophages in mammals [49].

TNF α production in plexiform lesions increases with lesion progression

To confirm that the development of plexiform lesions in our avian model is associated with aberrant TNF α production, an immunohistochemical study of histological sections was performed. As expected, the parent vessels of plexiform lesions had increased signal of TNF α in the endothelial cell layer than the vessels without lesions (Fig. 2A, B). In addition, we noted a progressive increase in stromal TNF α production with the lesion progression (Fig. 2C).

Chronic TNF α exposure promotes the differentiation of eEPCs to macrophages

Although TNF α has been shown to induce cell death in many cell types [50], we did not determine a significant effect of TNF α at 10–100 ng/ml on cell viability (Additional file 2: Fig. S1). Nevertheless, a remarkable morphologic change was observed in TNF α -challenged eEPCs, characterized by loss of the typical spindle-shaped eEPC appearance and acquisition of rounded and loosely attached phenotype showing numerous superficial dendrites (Fig. 3A), matching the morphology of mature macrophages. In line with the morphologic change, the portion of cells with an eEPC phenotype, as defined as acLDL+/lectin+ cells [18, 51], was markedly declined following exposure to TNF α for 6 days (Fig. 3B). In contrast, MRC1+ cells were significantly increased while CD133+ cells were decreased in the same cultures (Fig. 3C, D). To further confirm that chronic inflammation drives the differentiation of eEPCs to macrophage lineage, phagocytosis assay was performed. As shown in Fig. 3E, eEPCs acquired strong phagocytic capability in uptake of FITC-labeled bacteria following treatment with TNF α for 6 days. Together, the data suggest that chronic TNF α challenge triggers the differentiation of eEPCs to macrophages.

Chronic exposure to TNF α attenuates in vivo angiogenic potential of eEPCs

We next evaluated the effects of chronic TNF α exposure on the angiogenic potential of eEPCs by using an in vivo Matrigel plug assay. H&E staining revealed the presence of numerous luminal structures containing erythrocytes in the plugs with eEPCs; however, in the presence of TNF α , the number of vascular structures in the plugs containing eEPCs was significantly reduced (Fig. 4B–D). Of note, few host cells invaded the plugs containing Matrigel only or Matrigel with r-TNF α , although giant cells were found to infiltrate into the borders of the implants (Fig. 4A), indicating that eEPCs within the implants were not contaminated with host cells (Fig. 4B,

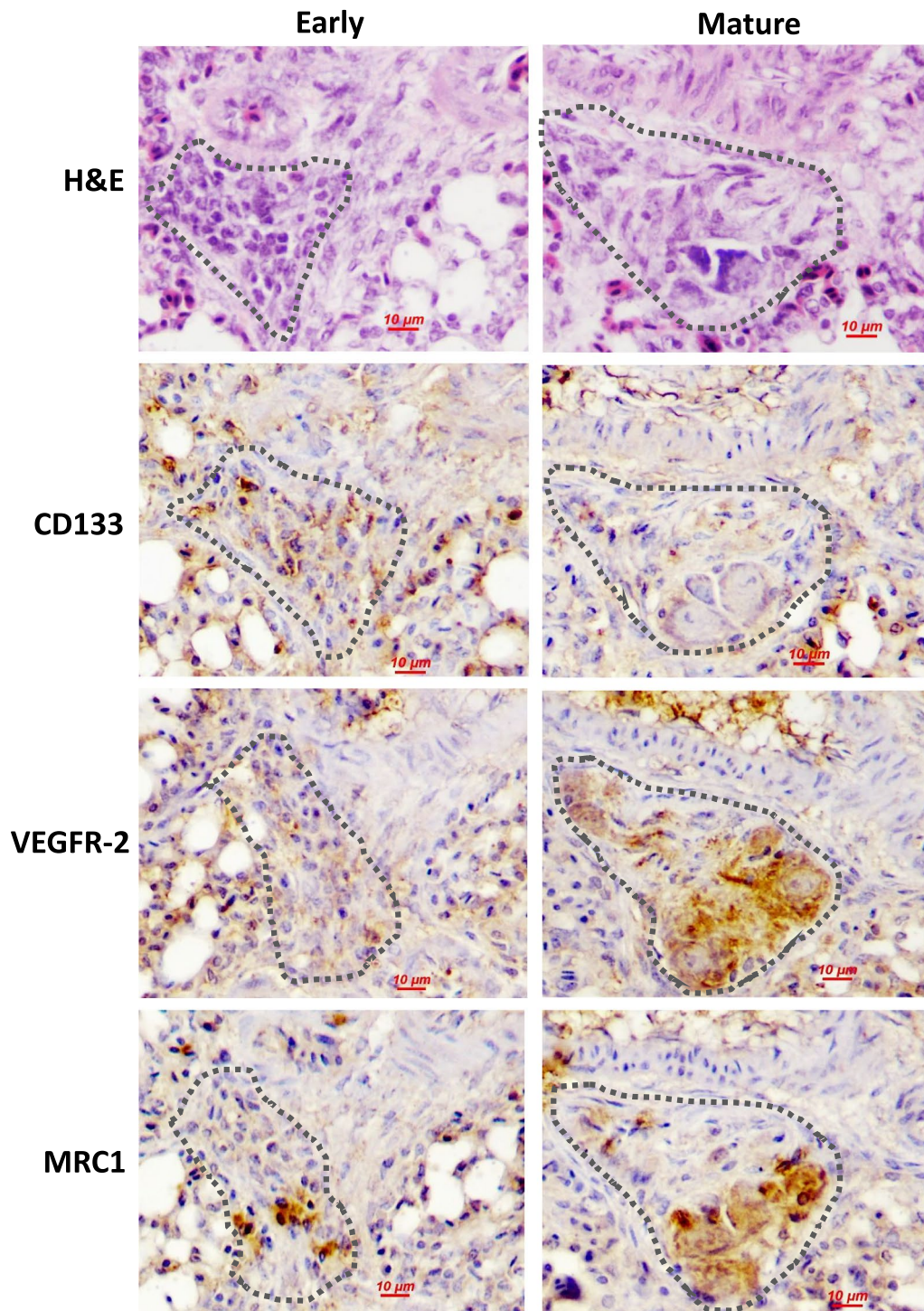


Fig. 1 Characterization of the phenotypes of cells within plexiform lesions. Representative serial hematoxylin and eosin (H&E)-stained sections and immunohistochemistry images showing histologic features and immunostaining results of plexiform lesions at different maturing stages from 4-week-old broiler chickens. The cells in the early immature lesion (left) exhibit endothelial-like morphology and those in more mature lesion (right) consist predominantly of foam-like macrophage cells. Immunohistochemistry analysis were performed using primary antibodies against monocyte/macrophage marker mannose receptor C-type 1 (MRC1), stem/progenitor cell marker CD133 and vascular endothelial growth factor receptor (VEGFR)-2. All immunostained sections are counterstained with hematoxylin. The dotted lines represent the edge of lesions

C). Plug sections were also subjected to immunohistochemistry analyses of the expression of MRC1 and CD133. Similar to the in vitro results, the Matrigel plugs containing TNF α and eEPCs had increased MRC1⁺ but decreased CD133⁺ cells than those containing eEPCs alone (Fig. 4E).

Nrf2 is essential for the phenotypic changes of eEPCs to macrophages in response to chronic TNF α stimulation

Nrf2 has been previously reported to regulate macrophage phenotype in response to oxidative stress and chronic inflammation [31]. On activation, Nrf2 translocates into the nucleus to exert a variety of biological functions [52]. To determine whether Nrf2 regulates phenotypic switching of eEPCs in response to chronic inflammation, we first determined by Western blot the protein level of Nrf2 in the cytoplasmic and nuclear fractions prepared from eEPCs after treatment with TNF α (50 ng/ml) for 3–6 days. As shown in Fig. 5A, Nrf2 protein was detected only in the nuclear fractions from both normal and TNF α -exposed cells. Interestingly, nuclear Nrf2 level tended to be decreased after treatment with TNF α for 3 days, followed by a marked increase at day 6. In line with the Western blot analysis, immunofluorescent staining demonstrated strongly increased nuclear Nrf2 signal in cells exposed to TNF α for 6 days (Fig. 5B).

To confirm Nrf2 overactivation drives phenotypic switching of eEPCs, we modulated Nrf2 activity in eEPCs by genetic knockdown of *Keap1*, which targets Nrf2 for ubiquitination and subsequent degradation in cytoplasm [53]. siRNA silencing of *Keap1* (Fig. 5C) resulted in a persistent activation of Nrf2, as evidenced by increased Nrf2 accumulation in the whole cell lysates and upregulated expression of its target gene *Nqo-1* (NAD(P)H:quinone oxidoreductase 1) (Fig. 5D). The effects of *Keap1* knockdown on *CD133* and *MRC1* expression were also evaluated. We noticed a marked upregulation in *CD133* mRNA level during the first 48 h following Nrf2 activation; however, an opposite effect was observed when Nrf2 activation was sustained for 72 h (Fig. 5E). Interestingly, *Keap1* knockdown resulted in a persistent upregulation in *MRC1* (Fig. 5F). Based on this finding, we hypothesized that Nrf2 regulates the promoter of *MRC1*. Results from dual luciferase reporter assay showed that

increasing chNrf2 plasmid upregulated the expression of the reporter gene carrying the promoter of *MRC1* in a dose-dependent manner, as evidenced by increased MRC1-luciferase activity (Fig. 5G). As expected, in the presence of TNF α , MRC1-luciferase activities in chNrf2-overexpressing cells were significantly enhanced. To confirm Nrf2 activation during the development of plexiform lesions, lung tissues were subjected to immunohistochemistry analysis (Additional file 3: Fig. S2). The immunostaining intensity for Nrf2 in mature lesions was stronger than that in early lesions. In addition, in contrast to the fact that Nrf2 was localized predominantly in the cytoplasm of cells in the early lesions, Nrf2 was found to be located predominantly in the nucleus of the foam-like macrophages present in more mature ones (Additional file 4: Fig. S3).

Intratracheal TNF α installation enhances the formation of plexiform lesions

As expected, local TNF α administration resulted in a significant increase in the number of plexiform lesions that were morphologically undistinguishable from those observed in the control group (Fig. 6A). Western blot analysis demonstrated increased amount of Nrf2 protein in the lung of TNF α -treated birds as compared to the controls, suggesting an overactivation of Nrf2 in response to TNF α (Fig. 6B). Consistent with the Western blot analysis data, birds treated with TNF α had increased endothelial Nrf2 expression as assessed by immunohistochemistry staining (Fig. 6C, D). TNF α administration also led to an elevation in RV/TV ratio, although the difference between groups was not statistically significant (Fig. 6E).

Discussion

In the present study, we described several findings supporting a view that eEPCs undergo macrophage differentiation during the development and evolution of plexiform lesions in our avian model. First, we have demonstrated that the cells in the early lesions have a typical eEPC phenotype (i.e., a mixed macrophage/endothelial cell phenotype) whereas those predominated in more mature lesions display molecular and morphological characteristics of macrophages. In addition, we show that

(See figure on next page.)

Fig. 2 Immunohistochemistry analysis of TNF α . **A** Normally branching vessels showed weak intimal expression of TNF α (right panel) while the arteries from which plexiform lesions arose displayed stronger endothelial signal of TNF α (left panel). NV normally branching vessels. PL plexiform lesion. **B** Semi-quantification analysis of TNF α in normally branching vessels (NV) and parent vessels of plexiform lesions (PVPL) by measuring the optical density. Data are expressed as median \pm 95% confidence interval of at least 20 arterioles. ****P** < 0.01. **C** The EPCs in early lesions (up) showed limited expression of TNF α as compared to the foam-like macrophage in mature lesions (down)

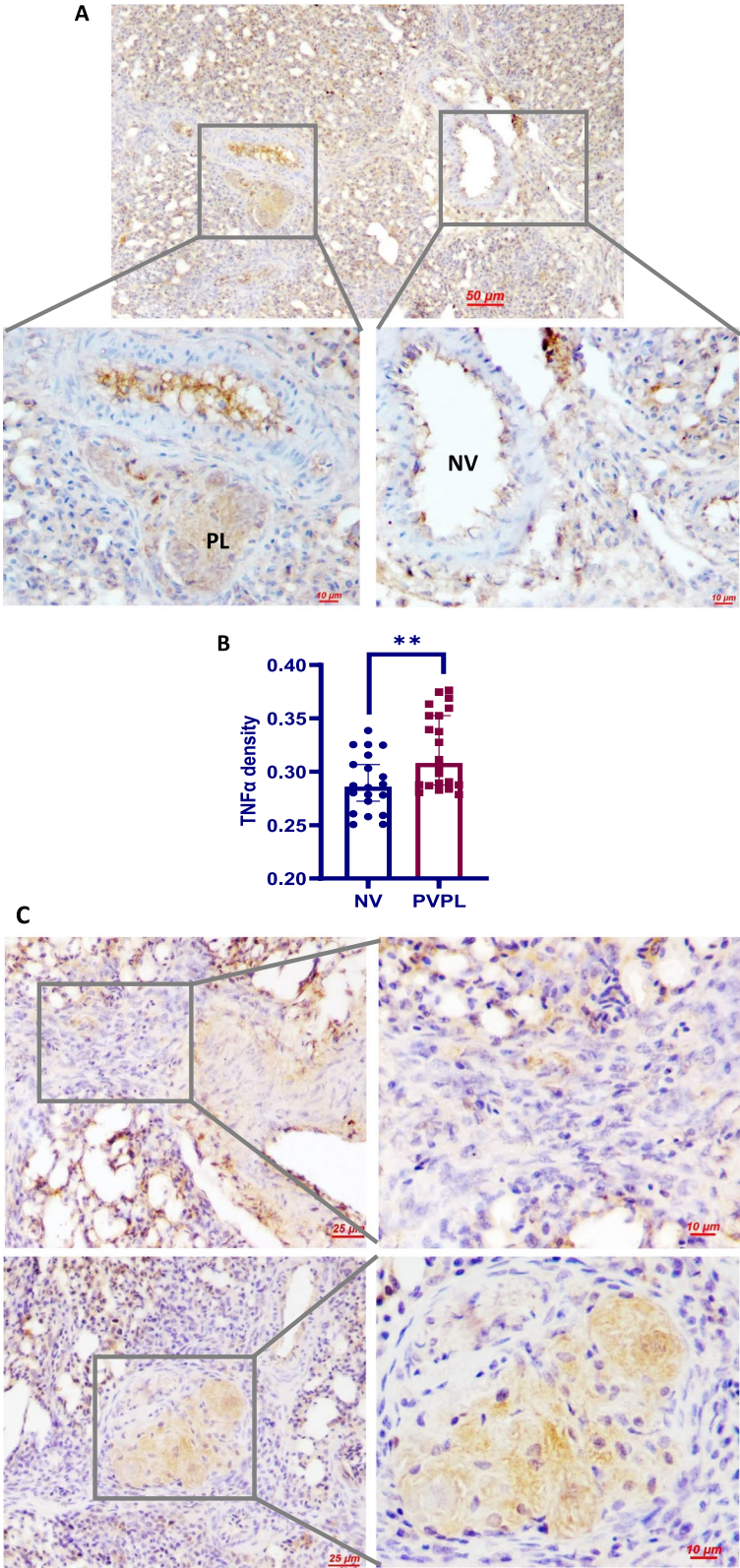


Fig. 2 (See legend on previous page.)

chronic inflammation induces the differentiation of eEPC into macrophage lineage, resulting in reduced angiogenic potential. Furthermore, we provide direct evidence that local administration of TNF α produces plexiform lesions. Our findings are important, regarding that the morphological and molecular characteristics and anatomic distributions of plexiform lesions developed in broilers closely resemble that seen in human PAH patients [34, 38].

PAH is a common cardiovascular disorder in modern broiler chickens, with an estimated incidence of 3% in all broilers reared under normal conditions that promote rapid growth. Although the primary triggers of PAH in broilers remain unclear, accumulating evidence suggests that anatomically insufficient lung volume predisposes broilers to PAH [54, 55]. Unlike that in mammals, avian pulmonary capillaries are rigid tubes that prevent them from expanding in response to increased blood flow. The result is that pulmonary arterial pressure rises linearly with pulmonary blood flow [56]. Rapid growth in broilers incurs progressive increases in cardiac output that inevitably lead to increased pulmonary arterial pressure due to the corresponding increases in pulmonary blood flow. Research has shown that pulmonary arterial pressure in normal broilers increases from 20 to 25 mmHg between 2 and 3 weeks and maintains at approximately 25 mmHg during weeks 4 and 5 of age [57]. Individuals having the most restricted pulmonary vascular capacity develop PAH when their right heart must develop an excessively elevated pulmonary arterial pressure to overcome the increased resistance to flow through the constricted pulmonary arterioles [55]. Sustained PAH triggers a series of events leading to structural vascular changes similar to the observations in human patients, including medial thickening and intimal proliferation [43, 58, 59]. Despite that fact that PAH broilers demonstrate increased plexiform lesions in their lungs [60], we and others have shown that PAH is not an essential prerequisite of the structures [38, 39, 42]. Nevertheless, an

elevation in pulmonary arterial pressure appears to play a role in the process [41]. It is now believed that increases in pulmonary arterial pressure may create turbulent flow in increasing numbers of branch points or curved portions, leading to increased plexiform lesions as observed in PAH broilers [60]. The importance of disturbed flow for the development of plexogenic pulmonary arteriopathy is indirectly supported by the fact that the lesions can hardly be recapitulated in rodents in which turbulent flow rarely occurs because of the rapid stabilization of flow in small vessels [61].

eEPCs have been recognized as monocyte-derived circulating angiogenic cells [18] and are known to home to the sites of vascular injury for endothelial repair [62]. We have previously reported the accumulation of eEPCs (CD133+ and VEGFR-2+ cells) in the early lesions located at branch points of interparabronchial arterioles in broiler lungs [42]. In the present study, we extended our previous findings by demonstrating the expression of a macrophagic marker MRC1 in these cells, further confirming their eEPC phenotype [63]. This finding is important, regarding the presence of fully differentiated macrophages in the mature lesions.

In compliance with the hypothesis that chronic inflammation contributes to the pathology of plexiform lesions, we determined increased endothelial TNF α expression in the parent arterioles of plexiform lesions and constant mononuclear cell infiltrates around the lesions. We next used an in vitro model to test our hypothesis that chronic inflammation induces macrophage differentiation of eEPC resulting in reduced angiogenic potential. In line with an early study where incubation with TNF α showed no effect on eEPC death [64], we did not observe a significant effect of TNF α at 10–100 ng on cell viability. As expected, prolonged TNF α stimulation promoted the differentiation of eEPCs to macrophages, as evidenced by decreased expression in CD133 and increased expression in MRC1 together with the acquisition of strong

(See figure on next page.)

Fig. 3 Chronic exposure to TNF α leads to eEPC-to-macrophage conversion. **A** Representative photographs showing the morphological change of eEPCs in response to chronic TNF α exposure. Cells were incubated with TNF α at 50 ng/ml for 6 days. **B** Characterization of eEPCs. eEPCs were subjected to fluorescence staining with Dil-ac-LDL (red) and lectin (green). Cell nuclei were visualized by DAPI (blue). Dual positives were counted ($n=3$). **C** Characterization of macrophage lineage. eEPCs were subjected to fluorescence staining with anti-KUL-01 (green). The cell nuclei were labeled with DAPI (blue). MRC1+ cells were counted ($n=6$). **D** eEPCs were exposed to TNF α at 50 ng/ml for 3–6 days and subjected to immunofluorescence analysis with anti-CD133 (green). The cell nuclei were labeled with DAPI (blue). CD133+ cells were counted ($n=6$). **E** Phagocytosis capability assay. eEPCs were exposed to TNF α at 50 ng/ml for 3–6 days and allowed to phagocytose *E. coli* (green). The cell nuclei were labeled with DAPI (blue). Chicken PBMC-derived macrophages were used as a positive control. Cells having intracellular bacteria were counted ($n=6$). The data are representative of 2 separate experiments. Photographs are from one representative experiment. Data were expressed as median \pm 95% confidence interval (Mann–Whitney). * $P < 0.05$. ** $P < 0.01$

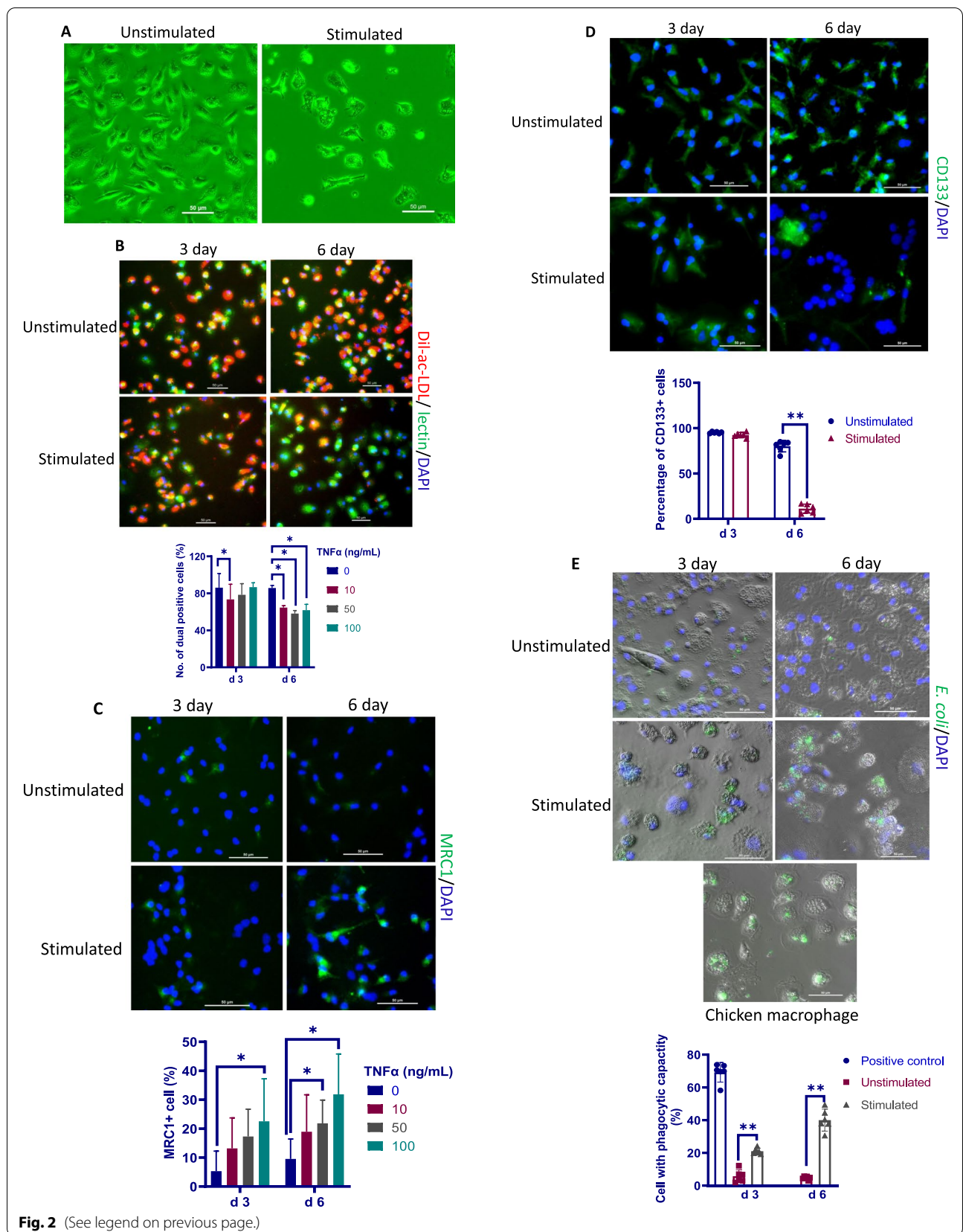


Fig. 2 (See legend on previous page.)

phagocytotic activity. Additional experiments were carried out to examine if chronic inflammation leads to a conversion of eEPCs to macrophages in vivo. For this, eEPCs were mixed with Matrigel containing TNF α and were subcutaneously injected into broiler chickens to allow neovascularisation to develop for 6 days. Results from these studies demonstrate that eEPCs undergo macrophage differentiation in Matrigel plugs containing TNF α , resulting in reduced neovascularization in Matrigel plugs. Together, the data provide clear evidence that chronic inflammation predisposes eEPCs to differentiate into macrophage lineage, a process that impairs the angiogenic potential of eEPCs. In context, our results allow us to argue that the development of plexiform lesions is attributed to the impairment of angiogenic processes that is associated with the switching of eEPCs to macrophages in response to chronic inflammation.

To explore the potential mechanisms by which TNF α promotes eEPC-to-macrophage conversion, we focused on Nrf2, a well-known oxidative stress-responsive transcription factor. Interestingly, TNF α exposure had no significant effect on Nrf2 activation in eEPCs during the first 3 days, suggesting an intrinsic capability of these cells to tolerate inflammatory stimulation [65]. However, Nrf2 activation was evident at day 6 following TNF α exposure, a time point at which increased MRC1+ macrophages were present in the cultures. We found that Nrf2 hyperactivation was sufficient to induce the differentiation of eEPC to macrophage lineage. In support of our findings, Nrf2 has also been shown to regulate the differentiation of other cell types [66, 67]. In addition, we found that Nrf2 was able to bind to the promoter of *MRC1* to trigger its expression. By using a luciferase assay, we confirmed that Nrf2 regulates TNF α -induced eEPC-to-macrophage conversion. Showing a very good agreement with the in vitro data, Nrf2 protein was found to be barely expressed in the cells within the early plexiform lesions, whereas its expression was strong in more mature ones. Taken together, it is reasonable to suggest

that local Nrf2 hyperactivation contributes to the pathogenesis of plexiform lesions by inducing macrophage differentiation of eEPCs. Further studies are warranted to test whether targeting Nrf2 would be beneficial for intervention of the lesions.

The present study has several limitations. First, since specific surface markers for the identification of macrophage subpopulations in avian species have not been defined, subgroups of the macrophages in the plexiform lesions and in the in vitro cultures challenged with TNF α were not specified. Second, the present study focused only on the eEPCs in the pathogenesis of plexiform lesions. We acknowledge that TNF α may also stimulate endothelial-to-mesenchymal transition to promote the process [68]. Third, we did not evaluate the effect of TNF α installation on pulmonary blood flow and pulmonary vascular resistance. Thus, we could not conclude that the moderate increase in pulmonary arterial pressure as measured by RV/TV ratio after TNF α administration is merely related to the increased formation of plexiform lesions.

Conclusions

In summary, the current study provides evidence supporting the view that local inflammatory cytokine TNF α plays a critical role in the development of plexiform lesions. Our observation that chronic exposure to TNF α promotes the phenotypic switching of eEPCs towards macrophage lineage might explain why the eEPCs lose their angiogenic activities after homing to the sites of vascular injury within the pulmonary vasculature and the origin of macrophages in the lesions. We show for the first time that Nrf2 drives the phenotypic switching of eEPCs towards macrophages following chronic TNF α stimulation. Taken together, understanding of these mechanisms that drive the development of plexiform lesions may pave the way to provide novel therapeutic strategies for the treatment of PAH patients.

(See figure on next page.)

Fig. 4 In vivo angiogenic potential and phenotype of eEPCs exposed to TNF α . **A–C** Representative photographs showing the morphology of subcutaneous Matrigel plug containing TNF α (blank control), eEPCs (control) and both (TNF α). Injection of eEPCs without TNF α led to the formation of capillary-like structures containing many erythrocytes. **D** Quantification of the newly-formed vessels in the Matrigel containing eEPCs with or without TNF α . Vessel density was expressed as the number of vessels per field ($\times 400$) ($n = 6$). **E** Immunohistochemical staining of paraffin-embedded Matrigel plug was performed by using the anti-KUL-01 and anti-CD133 antibody. Positive cells were automatically identified and counted in 6 randomly selected fields ($\times 400$) by using ImageJ (version 1.52). Bars are median \pm 95% confidence interval. The data are representative of 2 separate experiments

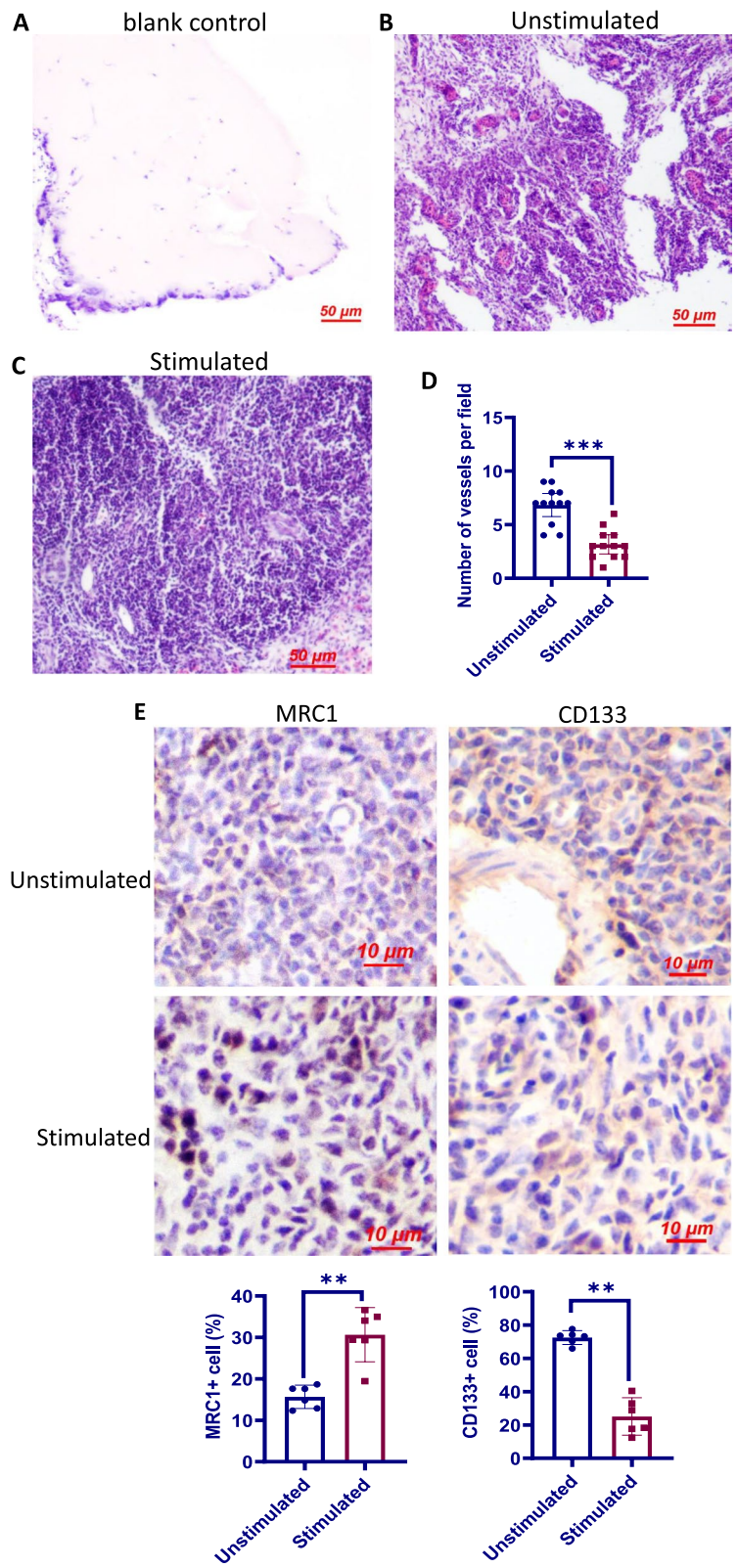


Fig. 4 (See legend on previous page.)

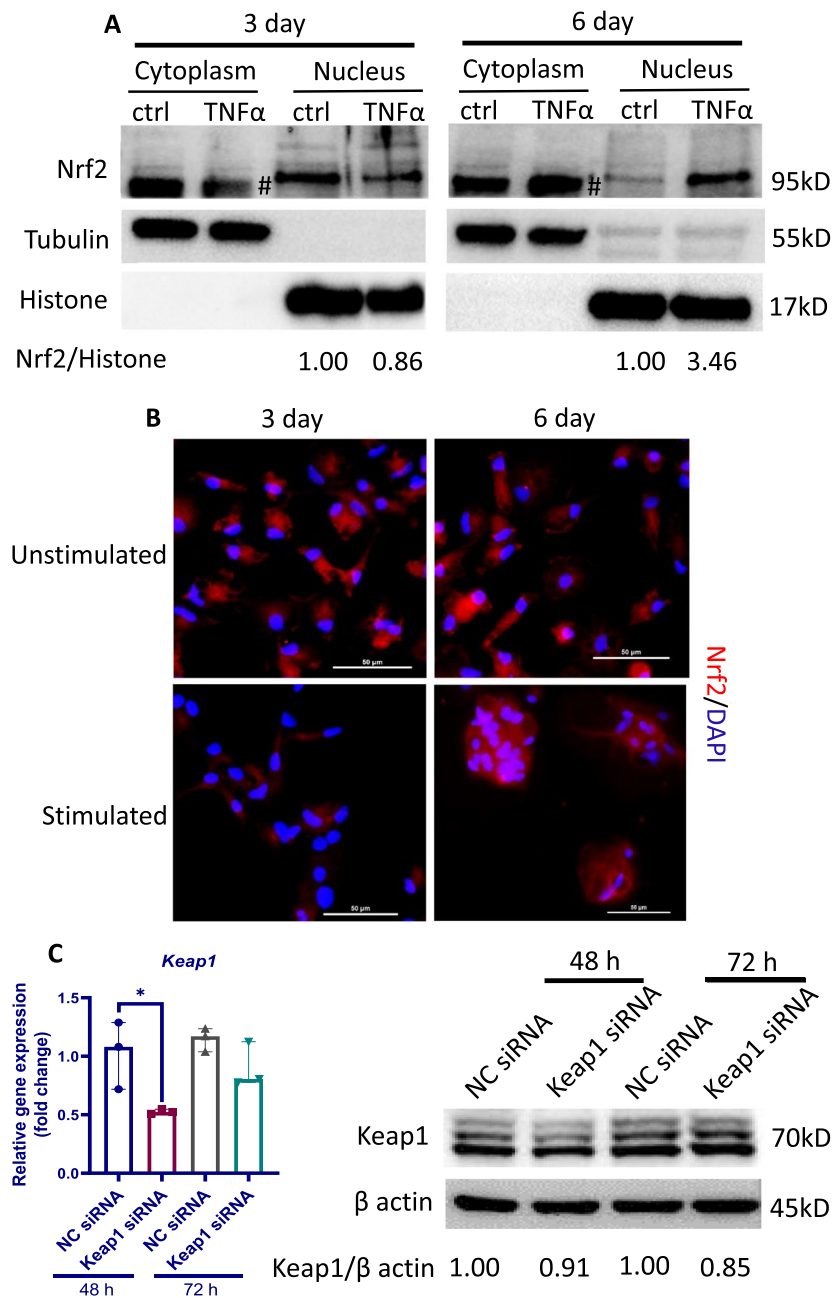


Fig. 5 Nrf2 regulates the eEPCs-to-macrophage conversion in response to chronic TNFα stimulation. **A** eEPCs were exposed to 50 ng/ml TNFα for the indicated time. Total cytoplasmic and nuclear proteins were extracted for Western blot using an anti-Nrf2. Tubulin and Histone are shown as loading control, respectively. # non-specific bands. **B** Alternatively, cells were subjected to immunofluorescence analysis of Nrf2 nuclear translocation. Nrf2 was probed with a primary anti-Nrf2 antibody and visualized with an Alexa Fluor 594-conjugated secondary antibody (red). Cell nuclei were stained with DAPI (blue). **C–F** eEPCs were transfected with a siRNA targeting chicken Keap1 or a negative control (NC) siRNA for 48–72 h. **C** Evaluation of knockdown efficiency of Keap1. Total RNAs and whole-cell lysates were subjected to qPCR and Western blot analysis, respectively, for determination of Keap1 mRNA (left panel, $n = 3$) and protein levels (right panel). **D** Evaluation of Nrf2 activation after siRNA silencing of Keap1. Total RNAs and whole-cell lysates were subjected to Western blot and qPCR analysis, respectively, for determination of Nrf2 protein levels (left panel) and relative mRNA level of Nrf2 target genes Nqo-1 (NAD(P)H:quinone oxidoreductase 1) (right panel, $n = 3$). **E–F** Effect of Nrf2 activation on the mRNA expression of stem/progenitor cell marker CD133 and macrophage marker MRC1 ($n = 3$). **G** HEK-293T cells were co-transfected with the chNrf2 expression vector pEGFP-C3-Nrf2 (denoted in μ g of DNA per well of a 12-well plate) and the plasmid constructs containing a firefly luciferase gene under the control of the MRC1 promoter along with the pRL-TK Renilla. Empty pEGFP-C3 was used as control. Cells were incubated with or without TNFα (50 ng/ml) for 72 h and processed for measurement of luciferase activity ($n = 3$). The data are representative of at least 2 separate experiments with similar results. Data were expressed as median \pm 95% confidence interval. * $P < 0.05$

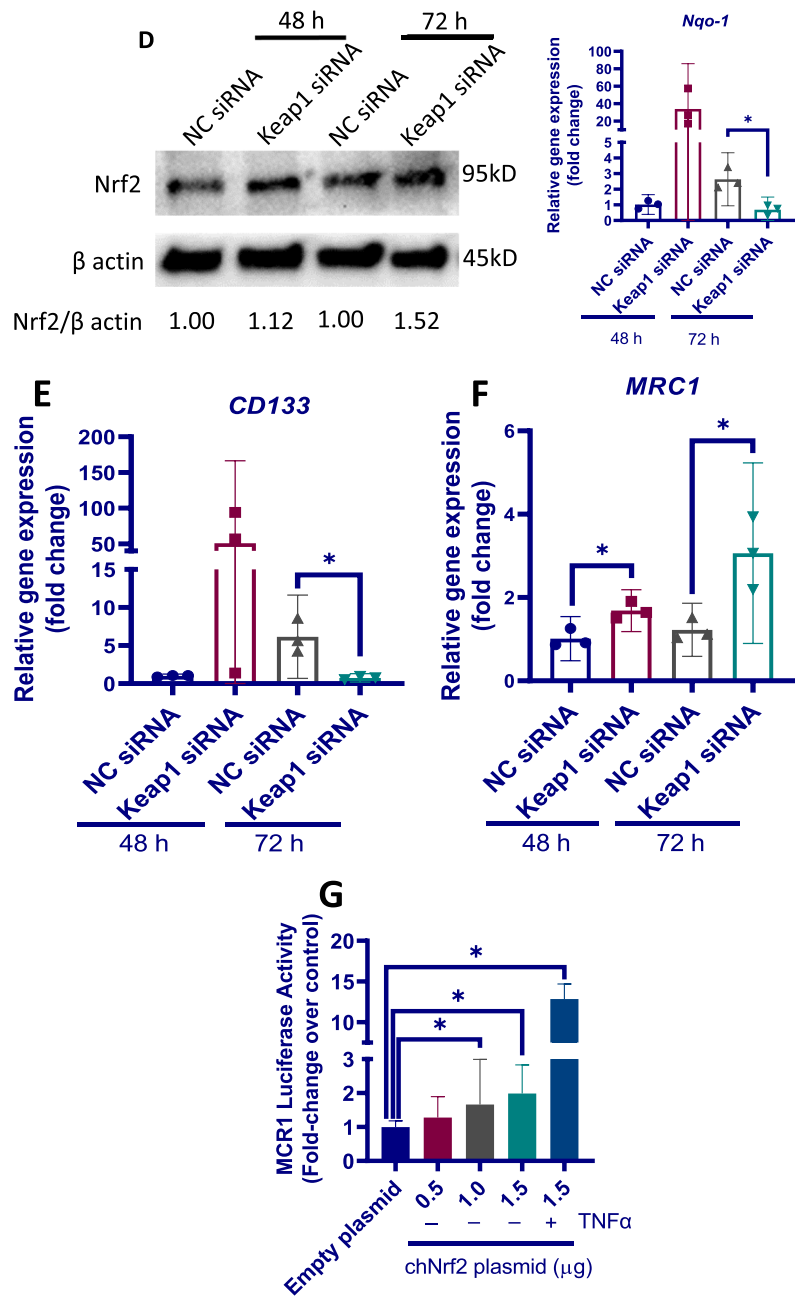


Fig. 5 continued

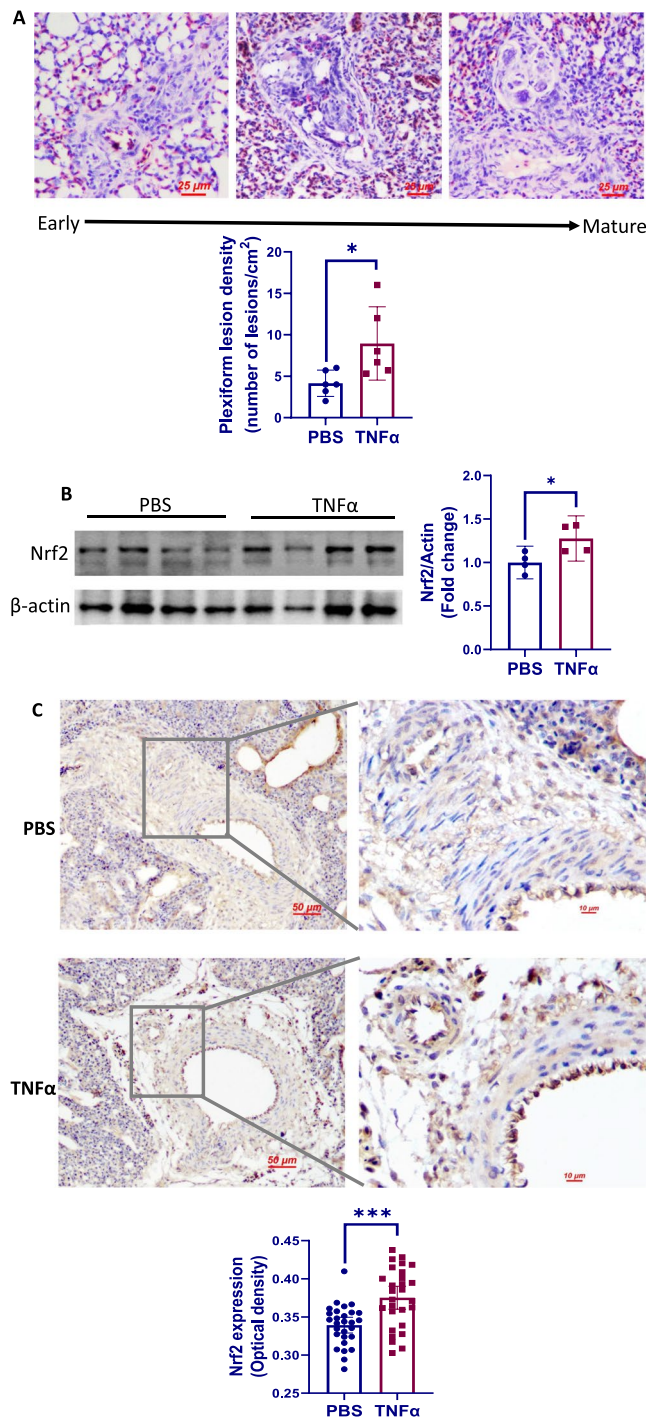


Fig. 6 Intratracheal TNF α installation enhances the formation of plexiform lesions. **A** Representative photographs showing the morphology of plexiform lesions in the lung of TNF α -treated birds. Plexiform lesion density was expressed as the number of lesions per section/cm² per section ($n = 6$). **B** Western blots and densitometry analyses of Nrf2. Total proteins extracted from lung tissue were analyzed by immunoblotting with anti-Nrf2 antibody. β -actin are shown as loading control. Densitometry data represent the mean \pm 95% confidence interval of 4 birds and are representative of 2 separate experiments. **C** Immunohistochemistry staining of Nrf2 in lung tissue. Expression of endothelial Nrf2 was semi-quantified by measuring the optical density (OD) in 28 pulmonary arterioles randomly selected from 6 birds in each group

Abbreviations

CAC: Circulating angiogenic cells; Dil-Ac-LDL: 1,1-Dioctadecyl-3,3,3,3-tetramethylindocarbocyanine-labelled acetylated low-density lipoprotein; eEPCs: Early progenitor endothelial cells; H&E: Haematoxylin and eosin; Keap1: Kelch-like ECH-associated protein 1; Lectin: *Ulex europaeus* agglutinin; Nqo-1: NAD(P)H:quinone oxidoreductase 1; Nrf2: Nuclear factor erythroid 2-related factor 2; PAH: Pulmonary arterial hypertension; PBMC: Peripheral blood mononuclear cell; TNF α : Tumor necrotic factor- α ; VEGFR-2: Vascular endothelial growth factor receptor-2.

Supplementary Information

The online version contains supplementary material available at <https://doi.org/10.1186/s12931-022-02210-7>.

Additional file 1: Table S1. Primers information.

Additional file 2: Fig. S1. Effect of TNF α on eEPC viability.

Additional file 3: Fig. S2. Nrf2 activation during the development of plexiform lesions.

Additional file 4: Fig. S3. The effect of TNF α administration on RV/TV ratio of broilers.

Acknowledgements

We thank Undergraduate Experimental Teaching Centre of College of Animal Sciences, Zhejiang University, for assistance in qPCR analysis.

Author contributions

FJS participated in the design of the study, collected samples, and was a major contributor in lab analysis. XLG participated in data collection, animal management, interpretation of the results. XT conceived the idea, supervised the experiment, and wrote the manuscript. RL contributed to data statistical analysis and manuscript writing. JXX and DYL contributed to data curation and validation. QHL, TZ and CF contributed to chicken management and sample collection. All authors read and approved the final manuscript.

Funding

This study was supported by the National Natural Science Foundation of China (Project No. 31872444) and the Key R & D Project of Zhejiang Province (Project No. 2020C02032).

Availability of data and materials

The datasets used and/or analysed during the current study are available from the corresponding author on reasonable request.

Declarations

Ethics approval and consent to participate

All the operation was approved by the Ethic's Committee of the Zhejiang University (Approved No. ZJU2015-445-12).

Consent for publication

Not applicable.

Competing interests

The authors declare no competing interests.

Author details

¹Department of Veterinary Medicine, Zhejiang University, Hangzhou 310058, People's Republic of China. ²Center for Veterinary Medicine, Zhejiang University, Hangzhou 310058, People's Republic of China. ³Institute of Preventive Veterinary Sciences, Zhejiang University, Hangzhou 310058, People's Republic of China. ⁴Department of Animal Sciences, Zhejiang University, Hangzhou 310058, People's Republic of China. ⁵Hainan Institute of Zhejiang University, Sanya, Hainan Province, People's Republic of China.

Received: 3 August 2022 Accepted: 4 October 2022

Published online: 23 October 2022

References

- Jonigk D, Golpon H, Bockmeyer CL, Maegel L, Hoepfer MM, Gottlieb J, Nickel N, Hussein K, Maus U, Lehmann U, et al. Plexiform lesions in pulmonary arterial hypertension composition, architecture, and microenvironment. *Am J Pathol*. 2011;179:167–79.
- Cool CD, Stewart JS, Werahera P, Miller GJ, Williams RL, Voelkel NF, Tuder RM. Three-dimensional reconstruction of pulmonary arteries in plexiform pulmonary hypertension using cell-specific markers. Evidence for a dynamic and heterogeneous process of pulmonary endothelial cell growth. *Am J Pathol*. 1999;155:411–9.
- Palevsky HI, Schloo BL, Pietra GG, Weber KT, Janicki JS, Rubin E, Fishman AP. Primary pulmonary hypertension. Vascular structure, morphometry, and responsiveness to vasodilator agents. *Circulation*. 1989;80:1207–21.
- Lee SD, Shroyer KR, Markham NE, Cool CD, Voelkel NF, Tuder RM. Monoclonal endothelial cell proliferation is present in primary but not secondary pulmonary hypertension. *J Clin Invest*. 1998;101:927–34.
- Yeager ME, Halley GR, Golpon HA, Voelkel NF, Tuder RM. Microsatellite instability of endothelial cell growth and apoptosis genes within plexiform lesions in primary pulmonary hypertension. *Circ Res*. 2001;88:E2–11.
- Ohta-Ogo K, Hao H, Ishibashi-Ueda H, Hirota S, Nakamura K, Ohe T, Ito H. CD44 expression in plexiform lesions of idiopathic pulmonary arterial hypertension. *Pathol Int*. 2012;62:219–25.
- Tuder RM, Groves B, Badesch DB, Voelkel NF. Exuberant endothelial cell growth and elements of inflammation are present in plexiform lesions of pulmonary hypertension. *Am J Pathol*. 1994;144:275–85.
- Fadini GP, Avogaro A. Cell-based methods for ex vivo evaluation of human endothelial biology. *Cardiovasc Res*. 2010;87:12–21.
- Fujisawa T, Tura-Ceide O, Hunter A, Mitchell A, Vesey A, Medine C, Gallogly S, Hadoke P, Keith C, Sproul A, et al. Endothelial progenitor cells do not originate from the bone marrow. *Circulation*. 2019;140:1524–6.
- Jones CP, Rankin SM. Bone marrow-derived stem cells and respiratory disease. *Chest*. 2011;140:205–11.
- Chong MS, Ng WK, Chan JK. Concise Review: Endothelial progenitor cells in regenerative medicine: applications and challenges. *Stem Cells Transl Med*. 2016;5:530–8.
- Walter DH, Rittig K, Bahlmann FH, Kirchmair R, Silver M, Murayama T, Nishimura H, Losordo DW, Asahara T, Isner JM. Statin therapy accelerates reendothelialization: a novel effect involving mobilization and incorporation of bone marrow-derived endothelial progenitor cells. *Circulation*. 2002;105:3017–24.
- Hristov M, Zernecke A, Bidzhekov K, Liehn EA, Shagdarsuren E, Ludwig A, Weber C. Importance of CXC chemokine receptor 2 in the homing of human peripheral blood endothelial progenitor cells to sites of arterial injury. *Circ Res*. 2007;100:590–7.
- Toshner M, Voswinckel R, Southwood M, Al-Lamki R, Howard LS, Marchesan D, Yang J, Suntharalingam J, Soon E, Exley A, et al. Evidence of dysfunction of endothelial progenitors in pulmonary arterial hypertension. *Am J Respir Crit Care Med*. 2009;180:780–7.
- Montani D, Perros F, Gambaryan N, Girerd B, Dorfmüller P, Price LC, Huertas A, Hammad H, Lambrecht B, Simonneau G, et al. C-kit-positive cells accumulate in remodeled vessels of idiopathic pulmonary arterial hypertension. *Am J Respir Crit Care Med*. 2011;184:116–23.
- Asosingh K, Aldred MA, Vasanthi A, Drazba J, Sharp J, Farver C, Comhair SA, Xu W, Licina L, Huang L, et al. Circulating angiogenic precursors in idiopathic pulmonary arterial hypertension. *Am J Pathol*. 2008;172:615–27.
- Gerasimovskaya E, Kratzer A, Sidiakova A, Salys J, Zamora M, Tarasiewicz-Stewart L. Interplay of macrophages and T cells in the lung vasculature. *Am J Physiol Lung Cell Mol Physiol*. 2012;302:L1014–22.
- Rehman J, Li J, Orschell CM, March KL. Peripheral blood “endothelial progenitor cells” are derived from monocyte/macrophages and secrete angiogenic growth factors. *Circulation*. 2003;107:1164–9.
- Zhang SJ, Zhang H, Wei YJ, Su WJ, Liao ZK, Hou M, Zhou JY, Hu SS. Adult endothelial progenitor cells from human peripheral blood maintain monocyte/macrophage function throughout in vitro culture. *Cell Res*. 2006;16:577–84.
- Cheng SM, Chang SJ, Tsai TN, Wu CH, Lin WS, Lin WY, Cheng CC. Differential expression of distinct surface markers in early endothelial progenitor cells and monocyte-derived macrophages. *Gene Expr*. 2013;16:15–24.
- Schmeisser A, Garlich CD, Zhang H, Eskafi S, Gaffy C, Ludwig J, Strasser RH, Daniel WG. Monocytes coexpress endothelial and macrophagocytic

- lineage markers and form cord-like structures in Matrigel under angiogenic conditions. *Cardiovasc Res*. 2001;49:671–80.
22. Lopes-Coelho F, Silva F, Gouveia-Fernandes S, Martins C, Lopes N, Domingues G, Brito C, Almeida AM, Pereira SA, Serpa J. Monocytes as endothelial progenitor cells (EPCs), another brick in the wall to disentangle tumor angiogenesis. *Cells-Basel*. 2020;9:107.
 23. Vinci MC, Piacentini L, Chiesa M, Saporiti F, Colombo GI, Pesce M. Inflammatory environment and oxidized LDL convert circulating human proangiogenic cells into functional antigen-presenting cells. *J Leukoc Biol*. 2015;98:409–21.
 24. Pervaiz S, Taneja R, Ghaffari S. Oxidative stress regulation of stem and progenitor cells. *Antioxid Redox Signal*. 2009;11:2777–89.
 25. Haneline LS. Redox regulation of stem and progenitor cells. *Antioxid Redox Signal*. 2008;10:1849–52.
 26. Baird L, Dinkova-Kostova AT. The cytoprotective role of the Keap1-Nrf2 pathway. *Arch Toxicol*. 2011;85:241–72.
 27. Cho HY, Reddy SP, Debiase A, Yamamoto M, Kleeberger SR. Gene expression profiling of NRF2-mediated protection against oxidative injury. *Free Radic Biol Med*. 2005;38:325–43.
 28. Cho HY, Reddy SP, Kleeberger SR. Nrf2 defends the lung from oxidative stress. *Antioxid Redox Signal*. 2006;8:76–87.
 29. Ma Q. Role of nrf2 in oxidative stress and toxicity. *Annu Rev Pharmacol Toxicol*. 2013;53:401–26.
 30. Murakami S, Motohashi H. Roles of Nrf2 in cell proliferation and differentiation. *Free Radic Biol Med*. 2015;88:168–78.
 31. Kadl A, Meher AK, Sharma PR, Lee MY, Doran AC, Johnstone SR, Elliott MR, Gruber F, Han J, Chen W, et al. Identification of a novel macrophage phenotype that develops in response to atherogenic phospholipids via Nrf2. *Circ Res*. 2010;107:737–46.
 32. Xu M, Li XX, Wang L, Wang M, Zhang Y, Li PL. Contribution of Nrf2 to atherogenic phenotype switching of coronary arterial smooth muscle cells lacking CD38 gene. *Cell Physiol Biochem*. 2015;37:432–44.
 33. Bonnet S, Provencher S, Guignabert C, Perros F, Boucherat O, Schermuly RT, Hassoun PM, Rabinovitch M, Nicolls MR, Humbert M. Translating research into improved patient care in pulmonary arterial hypertension. *Am J Respir Crit Care Med*. 2017;195:583–95.
 34. Wideman RJ, Hamal KR. Idiopathic pulmonary arterial hypertension: an avian model for plexogenic arteriopathy and serotonergic vasoconstriction. *J Pharmacol Toxicol Methods*. 2011;63:283–95.
 35. Wideman RF, Rhoads DD, Erf GF, Anthony NB. Pulmonary arterial hypertension (ascites syndrome) in broilers: a review. *Poult Sci*. 2013;92:64–83.
 36. Hamal KR, Wideman RF, Anthony NB, Erf GF. Differential expression of vasoactive mediators in microparticle-challenged lungs of chickens that differ in susceptibility to pulmonary arterial hypertension. *Am J Physiol Regul Integr Comp Physiol*. 2010;298:R235–42.
 37. Shao FJ, Ying YT, Tan X, Zhang QY, Liao WT. Metabonomics profiling reveals biochemical pathways associated with pulmonary arterial hypertension in broiler chickens. *J Proteome Res*. 2018;17:3445–53.
 38. Wideman RF, Hamal KR, Bayona MT, Lorenzoni AG, Cross D, Khajali F, Rhoads DD, Erf GF, Anthony NB. Plexiform lesions in the lungs of domestic fowl selected for susceptibility to pulmonary arterial hypertension: incidence and histology. *Anat Rec (Hoboken)*. 2011;294:739–55.
 39. Wideman RJ, Mason JG, Anthony NB, Cross D. Plexogenic arteriopathy in broiler lungs: evaluation of line, age, and sex influences. *Poult Sci*. 2015;94:628–38.
 40. Hamal KR, Erf GF, Anthony NB, Wideman RF. Immunohistochemical examination of plexiform-like complex vascular lesions in the lungs of broiler chickens selected for susceptibility to idiopathic pulmonary arterial hypertension. *Avian Pathol*. 2012;41:211–9.
 41. Tan X, Shao FJ, Fan GJ, Ying YT. Expression of angiogenic factors and plexiform lesions in the lungs of broiler and layer chickens: a comparison. *Poult Sci*. 2018;97:1526–35.
 42. Tan X, Juan FG, Shah AQ. Involvement of endothelial progenitor cells in the formation of plexiform lesions in broiler chickens: possible role of local immune/inflammatory response. *J Zhejiang Univ Sci B*. 2017;18:59–69.
 43. Shao F, Liu R, Tan X, Zhang Q, Ye L, Yan B, Zhuang Y, Xu J. MSC transplantation attenuates inflammation, prevents endothelial damage and enhances the angiogenic potency of endogenous MSCs in a model of pulmonary arterial hypertension. *J Inflamm Res*. 2022;15:2087–101.
 44. Bi S, Tan X, Ali SQ, Wei L. Isolation and characterization of peripheral blood-derived endothelial progenitor cells from broiler chickens. *Vet J*. 2014;202:396–9.
 45. Shah QA, Tan X, Bi S, Liu X, Hu S. Differential characteristics and in vitro angiogenesis of bone marrow- and peripheral blood-derived endothelial progenitor cells: evidence from avian species. *Cell Prolif*. 2014;47:290–8.
 46. Song E, Lu CW, Fang LJ, Yang W. Culture and identification of endothelial progenitor cells from human umbilical cord blood. *Int J Ophthalmol*. 2010;3:49–53.
 47. Salome RG, McCoy DM, Ryan AJ, Mallampalli RK. Effects of intratracheal instillation of TNF- α on surfactant metabolism. *J Appl Physiol*. 1985;2000(88):10–6.
 48. Yu K, Gu MJ, Pyung YJ, Song KD, Park TS, Han SH, Yun CH. Characterization of splenic MRC1(hi)MHCII(lo) and MRC1(lo)MHCII(hi) cells from the monocyte/macrophage lineage of White Leghorn chickens. *Vet Res*. 2020;51:73.
 49. Wheeler KC, Jena MK, Pradhan BS, Nayak N, Das S, Hsu CD, Wheeler DS, Chen K, Nayak NR. VEGF may contribute to macrophage recruitment and M2 polarization in the decidua. *PLoS ONE*. 2018;13: e191040.
 50. Kim YS, Morgan MJ, Choksi S, Liu ZG. TNF-induced activation of the Nox1 NADPH oxidase and its role in the induction of necrotic cell death. *Mol Cell*. 2007;26:675–87.
 51. Zhong Z, Umemura A, Sanchez-Lopez E, Liang S, Shalapur S, Wong J, He F, Boassa D, Perkins G, Ali SR, et al. NF- κ B restricts inflammasome activation via elimination of damaged mitochondria. *Cell*. 2016;164:896–910.
 52. Loboda A, Damulewicz M, Pyza E, Jozkowicz A, Dulak J. Role of Nrf2/HO-1 system in development, oxidative stress response and diseases: an evolutionarily conserved mechanism. *Cell Mol Life Sci*. 2016;73:3221–47.
 53. McMahon M, Itoh K, Yamamoto M, Hayes JD. Keap1-dependent proteasomal degradation of transcription factor Nrf2 contributes to the negative regulation of antioxidant response element-driven gene expression. *J Biol Chem*. 2003;278:21592–600.
 54. Lorenzoni AG, Anthony NB, Wideman RJ. Transpulmonary pressure gradient verifies pulmonary hypertension is initiated by increased arterial resistance in broilers. *Poult Sci*. 2008;87:125–32.
 55. Wideman RJ, Eanes ML, Hamal KR, Anthony NB. Pulmonary vascular pressure profiles in broilers selected for susceptibility to pulmonary hypertension syndrome: age and sex comparisons. *Poult Sci*. 2010;89:1815–24.
 56. West JB, Watson RR, Fu Z. Major differences in the pulmonary circulation between birds and mammals. *Respir Physiol Neurobiol*. 2007;157:382–90.
 57. Forman MF, Wideman RJ. Measurements of pulmonary arterial pressure in anesthetized male broilers at two to seven weeks of age. *Poult Sci*. 2000;79:1645–9.
 58. Tan X, Chai J, Bi SC, Li JJ, Li WW, Zhou JY. Involvement of matrix metalloproteinase-2 in medial hypertrophy of pulmonary arterioles in broiler chickens with pulmonary arterial hypertension. *Vet J*. 2012;193:420–5.
 59. Tan X, Pan JQ, Li JC, Liu YJ, Sun WD, Wang XL. L-Arginine inhibiting pulmonary vascular remodeling is associated with promotion of apoptosis in pulmonary arterioles smooth muscle cells in broilers. *Res Vet Sci*. 2005;79:203–9.
 60. Kluess HA, Stafford J, Evanson KW, Stone AJ, Worley J, Wideman RF. Intrapulmonary arteries respond to serotonin and adenosine triphosphate in broiler chickens susceptible to idiopathic pulmonary arterial hypertension. *Poult Sci*. 2012;91:1432–40.
 61. Cybulsky MI, Marsden PA. Effect of disturbed blood flow on endothelial cell gene expression: a role for changes in RNA processing. *Arterioscler Thromb Vasc Biol*. 2014;34:1806–8.
 62. Chen L, Ding ML, Wu F, He W, Li J, Zhang XY, Xie WL, Duan SZ, Xia WH, Tao J. Impaired endothelial repair capacity of early endothelial progenitor cells in hypertensive patients with primary hyperaldosteronism: role of 5,6,7,8-tetrahydrobiopterin oxidation and endothelial nitric oxide synthase uncoupling. *Hypertension*. 2016;67:430–9.
 63. Medina R, O'Neill CL, Sweeney M, Guduric-Fuchs J, Gardiner TA, Simpson DA, Stitt AW. Molecular analysis of endothelial progenitor cell (EPC) subtypes reveals two distinct cell populations with different identities. *BMC Med Genomics*. 2010;3:18.
 64. Seeger FH, Haendeler J, Walter DH, Rochwalsky U, Reinhold J, Urbich C, Rossig L, Corbaz A, Chvatchko Y, Zeiher AM, et al. p38 mitogen-activated protein kinase downregulates endothelial progenitor cells. *Circulation*. 2005;111:1184–91.
 65. He T, Peterson TE, Holmuhamedov EL, Terzic A, Caplice NM, Oberley LW, Katusic ZS. Human endothelial progenitor cells tolerate oxidative stress

due to intrinsically high expression of manganese superoxide dismutase. *Arterioscler Thromb Vasc Biol.* 2004;24:2021–7.

66. Hinoi E, Fujimori S, Wang L, Hojo H, Uno K, Yoneda Y. Nrf2 negatively regulates osteoblast differentiation via interfering with Runx2-dependent transcriptional activation. *J Biol Chem.* 2006;281:18015–24.
67. Dai X, Yan X, Wintergerst KA, Cai L, Keller BB, Tan Y. Nrf2: redox and metabolic regulator of stem cell state and function. *Trends Mol Med.* 2020;26:185–200.
68. Bell RD, White RJ, Garcia-Hernandez ML, Wu E, Rahimi H, Marangoni RG, Slattery P, Duemmel S, Nuzzo M, Huertas N, et al. Tumor necrosis factor induces obliterative pulmonary vascular disease in a novel model of connective tissue disease-associated pulmonary arterial hypertension. *Arthritis Rheumatol.* 2020;72:1759–70.

Publisher's Note

Springer Nature remains neutral with regard to jurisdictional claims in published maps and institutional affiliations.

Ready to submit your research? Choose BMC and benefit from:

- fast, convenient online submission
- thorough peer review by experienced researchers in your field
- rapid publication on acceptance
- support for research data, including large and complex data types
- gold Open Access which fosters wider collaboration and increased citations
- maximum visibility for your research: over 100M website views per year

At BMC, research is always in progress.

Learn more biomedcentral.com/submissions

